Research Article/Generic Engineering

http://doi.org/10.15446/ing.investig.106659

Development and Validation of an Affordable Calibration Method for Surface Plates

Desarrollo y validación de un método de calibración asequible para superficies de referencia

Daniela I. Garzón[1], Jorge L. Galvis[2], David A. Plazas[3], Victor H. Gil[4], and Ovidio Almanza[5]

ABSTRACT

The measurement and calibration of flat surfaces is highly relevant for precision engineering, length metrology, and optical systems. Hence, many National Metrology Institutes (NMIs) tend to offer calibration services in this regard. Typically, mechanical, electromechanical, and optical measuring techniques are applied, with uncertainties in the order of micrometers. However, these techniques necessitate expensive equipment that requires periodical calibration and maintenance, which not many laboratories can afford. This work presents the validation of an affordable and simple calibration technique for surface plates through the evaluation of metrological compatibility with a reference calibration method. A surface plate was calibrated with both methods under the same conditions to validate our proposal. The 2.9 μm uncertainty obtained with the new method demonstrates its reliability and usability for laboratories with surface plates up to 300 mm in length that have a grade AA to B flatness accuracy. Due to its low initial cost, reliability, and ease of implementation, the proposed calibration method can be recommended to all laboratories and industries that need to constantly verify their surface plates.

Keywords: length metrology, surface plates, flatness

RESUMEN

La medición y calibración de superficies planas es de gran relevancia para la ingeniería de precisión, la metrología de longitud y los sistemas ópticos. Por lo tanto, muchos Institutos Nacionales de Metrología (NMIs) tienden a ofrecer servicios de calibración en este aspecto. Típicamente se aplican técnicas de medición mecánica, electromecánica y óptica, con incertidumbres del orden de micrómetros. Sin embargo, estas técnicas requieren de equipos costosos que necesitan calibración y mantenimiento periódicos, lo cual no es asequible para muchos laboratorios. Este trabajo presenta la validación de una técnica de calibración asequible y sencilla para placas de superficie mediante la evaluación de la compatibilidad metrológica con un método de calibración de referencia. Una placa de superficie fue calibrada con ambos métodos bajo las mismas condiciones para validar nuestra propuesta. La incertidumbre de 2.9 μm obtenida con el nuevo método demuestra su fiabilidad y usabilidad para laboratorios con placas de superficie de hasta 300 mm de longitud que tienen una precisión de planitud de grado AA a B. Debido a su bajo costo inicial, fiabilidad y facilidad de implementación, se puede recomendar el método de calibración propuesto a todos los laboratorios e industrias que necesiten verificar constantemente sus placas de superficie.

Palabras clave: metrología de longitud, superficies de referencia, planitud

Received: January 10th 2023
Accepted: April 24th 2024

Introduction

A surface plate can regarded as the initial point for most calibrations using precise dimensional and geometrical measurement instruments. Most laboratories, workshops, and industries have granite, steel, or ceramic surface plates, making the calibration of these surfaces an important task for dimensional metrology. The periodic calibration of surface plates typically occurs in intervals from six months to a year, depending on the grade, resistance, conditions, and frequency of use. Since surface plates have become a primary tool for dimensional laboratories, many methods have been developed to measure their flatness and straightness, such as the two-point connecting method (given i=K., n.d.), the Moody method (Moody, 1955), multi-point methods (Lakota and Gorog, 2011; Mikó, 2021), and scanning methods (Lakota and Gorog, 2011; Ju HUO, 2018; Ehret *et al.*, 2011; Schulz, Ehret, and Křen, 2013). Measurement can be performed with different devices, such as laser interferometers (Azaryan *et al.*, 2017; Ehret, Reinsch, and Schulz, 2019), electronic levels (Yellowhair and Burge, 2008; Glubokov, Glubokova, Afonina, Zelensky, and Semenishchev, 2022), spirit levels (Yang, Wang, and Zhu, 2021), autocollimators (Geckeler *et al.*, 2022; Heikkinen, Byman, Palosuo, Hemming, and Lassila, 2017), and coordinate measuring machines (CMMs) (Ali and Buajarern, 2013). Many of these works have achieved different levels of accuracy due to their main measurement principle, as is the case of the methods that use optical techniques such as interferometry or CMMs.

[1]BSc Physics, Unisersidad Nacional de Colombia, Colombia. E-mail: digarzonp@unal.edu.co
[2]Physics engineer, Universidad Nacional de Colombia, Colombia. MSc Physics, Universidad Nacional de Colombia, Colombia. Affiliation: Specialized professional, Instituto Nacional de Metrología, Colombia. E-mail:jlgalvis@inm.gov.co
[3]Mechanical engineer, Universidad Antonio Nariño, Colombia. Affiliation: Bachelor professional, Instituto Nacional de Metrología, Colombia. E-mail: daplazas@inm.gov.co
[4]Mechanical engineer, Fundación Universidad de America, Colombia. Affiliation: Specialized professional, Instituto Nacional de Metrología, Colombia. E-mail: vgil@inm.gov.co
[5]PhD Physics, Universidad de Valladolid, Spain. MSc Physics, Universidad Nacional de Colombia, Colombia. Affiliation: Associate professor, Universidad Nacional de Colombia, Colombia. E-mail: oaalmanzam@unal.edu.co

However, these techniques have many disadvantages, *e.g.*, the time required for a full surface plate calibration due to the alignment of the lasers or the uncertainty of the CMMs associated with the mechanical positioning system. In light of the above, the Moody method, coupled with the use of electronic levels, is the most commonly used calibration technique for surface plates. When an electronic level is employed for surface plate calibration, the measuring device is moved over a grid that is traced over the surface. Straightness is measured for each grid line, and the results are combined into a plane to represent the flatness deviations of the surface. However, interferometers, CMMs, and electronic levels are expensive for many factories and laboratories to obtain and maintain in the long term, causing them to look for onsite calibrations provided by NMIs. This work presents and validates the roto-translation method for flatness calibration on surface plates. The traditional Moody method using electronic levels was implemented to validate the results. The accuracy of the electronic levels and the similarity between the methods allowed for a direct comparison (Meijer and Heuvelman, 1990; Gusel, Acko, and Sostar, 2000a, 2000b). Thus, this work proposes an affordable method for the calibration of surface plates.

Calibration method

Many flatness calibration methods use the eight-line grid pattern proposed by Moody in 1955 (Moody, 1955; Drescher, 2003). All readings from the grid-line pattern form a mathematical surface to describe the flatness deviations of the points selected in a surface plate of interest. However, in the measuring process, each grid line has a different height as a consequence of variations in the initial point of each grid line used as reference to measure the deviations of the remaining points. Therefore, each grid line has to be mathematically treated to form a surface that describes the flatness deviations of the plate. This surface is delimited by three parallel planes: the first is called *roof plane* and is located at the same height as the highest deviation of the surface plate; the second is the *base plane* and is located at the same height as the lowest deviations of the surface plate; and the third is called *datum plane* and is located between the roof and the base planes (Figure 1). Usually, the calibration methods derived from Moody use the two diagonals of the grid line to form a reference plane for the rest of the lines. This plane is formed by the four ends and the intersection point of the two diagonals in the center of the surface plate.

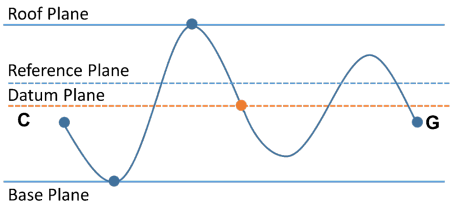

Figure 1. Identification of the principal planes for flatness calibration **Source:**Authors

The calibration method presented in this work is called *roto-translation* and is derived from the Moody method.

Roto-translation method

The roto-translation method divides the surface plate into an eight-line grid. The measurement points must be equally spaced along the lines, with a minimum of five points for each one. The grid includes four perimeter lines, two diagonals and two central ones (Figure 2).

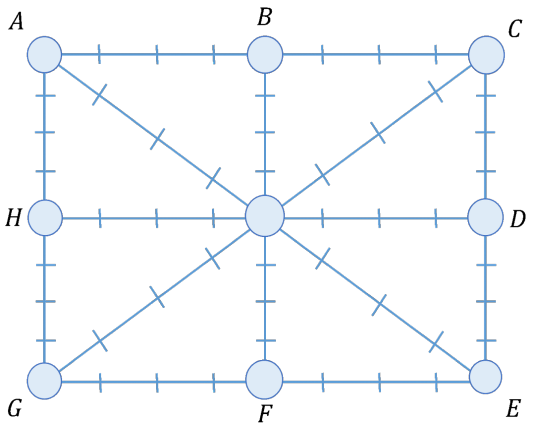

Figure 2. Grid line diagram **Source:** Authors

The calibration setup for this method uses a pin gauge set from 4.9 to 5.1 mm with increments of 0.001 mm per pin, two 5 mm gauge blocks to generate a GAP between the surface plate, and a steel precision straight edge, as shown in Figure 3.

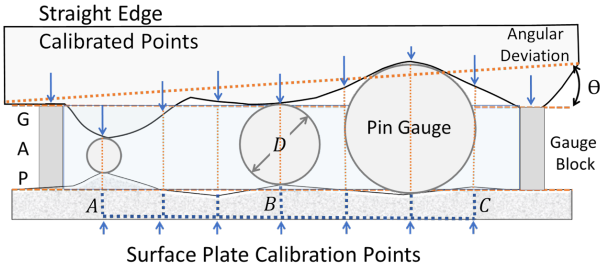

Figure 3. Roto-translation calibration setup **Source:** Authors

Figure 3 shows the measurement setup for surface plate calibration. This setup requires placing the two-gauge block outside the calibration line at the same distance from its limits, placing the straight edge over the gauge blocks and aligning each point of the edge with the calibration points traced on the surface plate. As the gap between the surface and the straight edge is expected to be 5 mm (*i.e.*, the length of the gauge blocks), any deviation from this value will be caused by the straight edge or the surface. As shown in Figure 3, any deviations in the straight edge affect the results of the calibration, causing two important issues: i) the angular deviation caused by the points used to support the edge over the gauge blocks and ii) the effect of the deviations of the straight edge on the readings taken with the gauge pins along the calibration path. In order to solve these issues, the straight edge-calibrated points have to be properly numbered and marked, thereby enabling proper corrections to measurement results. Finally, the accuracy of any measurement will depend on the stability of the setup and the care taken during calibration, as any misalignment

concerning the straight edge and the surface plate will introduce errors into the readings.

Methodology. The general procedure for this surface plate calibration technique is derived from Moody's method, but, instead of taking measurements by steps or stations, the straightness deviation of each grid line is taken directly from each measurement. This procedure is presented below.

1. Align the points of the straight edge with the calibration points of the surface and establish a direction of calibration (*e.g.*, from A to E). Then, center a 5 mm pin between the first point of the straight edge and the point of the surface plate, in order to measure the height of the gap G. If the pin does not fit, smaller pins have to be placed in a sequential manner until one fits in the gap (Figure 3). Otherwise, if the 5 mm pin is smaller than the gap, larger pins have to be placed until one fits. It is important to note that the smaller the increments or decrements of the pins, the more precise and accurate the measurements will be.

2. Store the readings, specifying the number of the straight edge point used for measuring each surface plate point, and classify them based on the two diagonals, the four-perimeter lines, and the two central lines. These readings are the combination between the deviation of the surface plate, the deviations of the straight edge, and the possible tilt of the straight edge caused by the height difference between the supporting points. For the sake of simplicity, the stored readings of each grid line are represented as a linear vector. This is shown in Equations (1), (2), and (3).

$$AE = \begin{bmatrix} x_0 \\ x_1 \\ \vdots \\ x_N \end{bmatrix} CG = \begin{bmatrix} x_0 \\ x_1 \\ \vdots \\ x_N \end{bmatrix} \tag{1}$$

$$AC = \begin{bmatrix} x_0 \\ x_1 \\ \vdots \\ x_N \end{bmatrix} CE = \begin{bmatrix} x_0 \\ x_1 \\ \vdots \\ x_N \end{bmatrix} GE = \begin{bmatrix} x_0 \\ x_1 \\ \vdots \\ x_N \end{bmatrix} AG = \begin{bmatrix} x_0 \\ x_1 \\ \vdots \\ x_N \end{bmatrix} \tag{2}$$

$$BF = \begin{bmatrix} x_0 \\ x_1 \\ \vdots \\ x_N \end{bmatrix} HD = \begin{bmatrix} x_0 \\ x_1 \\ \vdots \\ x_N \end{bmatrix} \tag{3}$$

3. To eliminate the influence of the straight edge on all the stored readings, make a vector SE that represents the deviations of the points along of the straight edge used for measuring each grid line, including the supporting points that are aligned with the gauge blocks. Then, translate the vector to its datum line by subtracting the deviation of the first point of the vector, as presented in Equation (4).

$$SE'_i = x_i - x_0 = x'_i \text{ for i = 0 to N} \tag{4}$$

As a consequence of the translation, the first value of the vector SE' is $x'_0 = 0$. Afterwards, rotate the vector as suggested in Equation (5) to eliminate the tilt caused by placing the straight edge over the gauge blocks.

$$SE''_i = x'_i + \left(x'_0 - x'_N\right)(i/N) = x''_i \text{ for i = 0 to N} \tag{5}$$

Both ends of the rotated vector SE'' will be $x''_0 = x''_N = 0$ (Figure 4).

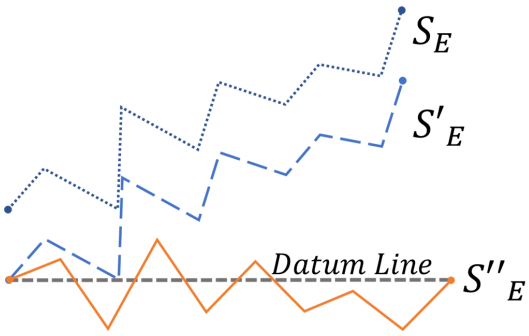

Figure 4. Translation and rotation of the vector of the straight edge **Source:** Authors

As a consequence of the translation and rotation of vector SE, the points of the edge will suffer a horizontal displacement with respect to their original position. In a geometrical analysis of this case, it was found that the maximum permissible horizontal displacement of the straight edge points is $\pm 1\mu m$ with respect to their original position, and that their maximum permissible straightness deviation is $\pm 40\mu m$. If the horizontal displacement of the straight edge points exceeds the $\pm 1\mu m$ interval, it is proven that, due to the alignment with respect to the points of the surface plate, the error in the readings increases. After the rotation, the gap formed by the gauge blocks at the supporting points will be 5 mm.

4. Based on Figure 4, the rotated vector SE'' will only consider the deviations of the straight edge around the datum line. To obtain the real deviation d at each calibration point of the surface plate, the deviations of SE'' have to be added to or subtracted from the diameter D of the pin that fit in the gap G between the surfaces (Figure 5).

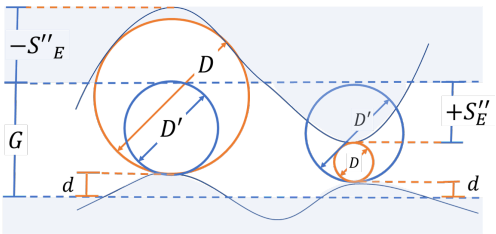

Figure 5. Corrections to the measurements taken with the gauge pins **Source:** Authors

Here, $-S''_E$ and $+S''_E$ are the deviations inward and outward of the edge, respectively, and D' is the real diameter of the pin, calculated as $D' = D + S''_E$ and $D' = D - S''_E$. Thus, the deviation at each point of the surface plate is $d = G - D'$. This correction has to be done for every point of the grid line in Figure 2.

5. Proper measurement of the two diagonals is of great importance since they establish the reference plane on which the rest of the grid lines is laid. After correcting the measurement readings, rotate both diagonals AE and CG until both their ends have the same deviation. To this effect, use Equation (6).

$$\begin{aligned} AE_i^r &= x_i + (x_0 - x_N)\,(i/N) = x^r{}_i \text{ for i = 0 to N} \\ CG_i^r &= x_i + (x_0 - x_N)\,(i/N) = x^r{}_i \text{ for i = 0 to N} \end{aligned} \tag{6}$$

where $x_0^r = x_N^r = \alpha^r$ for CG^r and $x_0^r = x_N^r = \beta^r$ for AE^r. Subsequently, translate the center of both diagonals to the datum plane by subtracting the deviation of the central point of each vector AE^r and CG^r, as shown in Equation (7).

$$\begin{aligned} AE_i'' &= x_i^r - x_{N/2}^r = x''{}_i \text{ for i = 0 to N} \\ CG_i'' &= x_i^r - x_{N/2}^r = x_i'' \text{ for i = 0 to N} \end{aligned} \tag{7}$$

Due to the translations, $x_0'' = x_N'' = \alpha, x_{N/2}'' = 0$ for CG'' and $x_0'' = x_N'' = \beta, x_{N/2}'' = 0$ for AE''. After the rotation and translation of the diagonals, they will form a reference plane for the rest of grid lines, which have to be rotated and translated to coincide with this plane. It is important to make a diagram with the values found for the center and both ends of the diagonals, as shown in Figure 6.

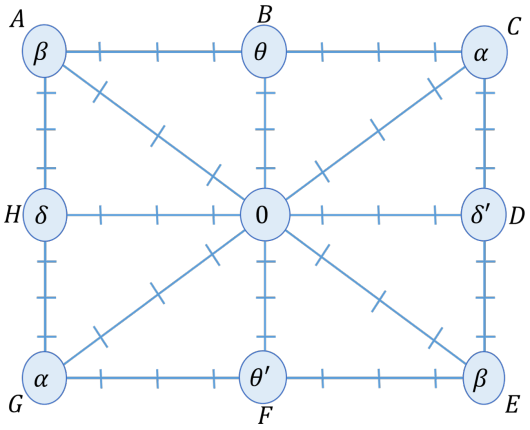

Figure 6. Diagram guide for the rotation and translation of grid lines **Source:** Authors

This diagram provides a guide for the operations that have to be performed in order to make all the grid lines coincide on the datum plane.

6. To make them coincide with the diagonals, translate the perimeter lines to the datum plane by subtracting their first values, as shown in Equation 8.

$$\begin{aligned} AC_i' &= x_i - x_0, \text{ for } i = 0 \text{ to } N \\ CE_i' &= x_i - x_0, \text{ for } i = 0 \text{ to } N \\ GE_i' &= x_i - x_0, \text{ for } i = 0 \text{ to } N \\ AG_i' &= x_i - x_0, \text{ for } i = 0 \text{ to } N \end{aligned} \tag{8}$$

Then, translate and rotate the perimeter lines to make them match at both ends with the diagonals. Equation (9) presents two roto-translation factors, $k_{\alpha\beta}$ and $k_{\beta\alpha}$, for the rotation and translation of each perimeter line that has to begin in α and end in β and of those that have to begin in β and end in α. To translate and rotate each perimeter line, use the roto-translation factor as indicated in Equation (10).

$$\begin{aligned} k_{\alpha\beta} &= \left[\alpha - \left(\beta - x_N'\right)\right]/N \\ k_{\beta\alpha} &= \left[\beta - \left(\alpha - x_N'\right)\right]/N \end{aligned} \tag{9}$$

$$\begin{aligned} AC_i'' &= x_i' + \left[\left(\alpha - x_N'\right) + \left(k_{\beta\alpha} \cdot (N - i)\right)\right] \\ AG_i'' &= x_i' + \left[\left(\alpha - x_N'\right) + \left(k_{\beta\alpha} \cdot (N - i)\right)\right] \\ CE_i'' &= x_i' + \left[\left(\beta - x_N'\right) + \left(k_{\alpha\beta} \cdot (N - i)\right)\right] \\ GE_i'' &= x_i' + \left[\left(\beta - x_N'\right) + \left(k_{\alpha\beta} \cdot (N - i)\right)\right] \end{aligned} \tag{10}$$

It is important to note that the roto-translation factors will be different for each perimeter line due to their dependence on the last value of each line x_N'. These rotations and translations position the perimeter lines onto the datum plane (Figure 6).

7. Subsequently, translate the central lines to the datum plane, as presented in Equation (11).

$$\begin{aligned} BF_i' &= x_i - x_0, \text{ for } i = 0 \text{ to } N \\ HD_i' &= x_i - x_0, \text{ for } i = 0 \text{ to } N \end{aligned} \tag{11}$$

Then, translate and rotate the central lines to make them coincide with the central deviation of the perimeter lines (Figure 6). As in the previous step, use the roto-translation factors $k_{\theta\theta'}$ and $k_{\delta\delta'}$, presented in Equations (12) and (13), to rotate and translate the central lines.

$$\begin{aligned} k_{\theta\theta'} &= \left[\theta - \left(\theta' - x_N'\right)\right]/N \\ k_{\delta\delta'} &= \left[\delta - \left(\delta' - x_N'\right)\right]/N \end{aligned} \tag{12}$$

$$\begin{aligned} BF_i'' &= x_i' + \left[\left(\theta' - x_N'\right) + \left(k_{\theta\theta'}.(N - i)\right)\right] \\ HD_i'' &= x_i' + \left[\left(\delta' - x_N'\right) + \left(k_{\delta\delta'}(N - i)\right)\right] \end{aligned} \tag{13}$$

If everything is done correctly, the middle point of the central lines should be zero. However, Moody established a closure error for the middle point of the central lines, which allows for a maximum deviation of 2.5 μm from 0 (Moody, 1955). When the absolute value of the deviations of the middle points of the central lines is greater than 0 and smaller than 2.5 μm, the central lines BF_i'' and HD_i'' have to be corrected, with the exception of both ends. To correct the central lines, subtract the deviation of the middle point from each central line.

8. Translate all the lines to the reference plane by subtracting the lowest value x_L'' of all grid lines, as shown in Equation (14).

$$\begin{aligned} AE_i^f &= x_i'' - x_L'' = x_i^f \quad CE_i^f = x_i'' - x''_L = x_i^f \\ CG_i^f &= x_i'' - x_L'' = x_i^f \quad GE_i^f = x_i'' - x''_L = x_i^f \\ AC_i^f &= x_i'' - x_L'' = x_i^f \quad BF_i^f = x_i'' - x_L'' = x_i^f \\ AG_i^f &= x_i'' - x_L'' = x_i^f \quad HD_i^f = x_i'' - x_L'' = x_i^f \end{aligned} \tag{14}$$

Finally, all the grid lines will coincide on the reference plane and represent the flatness deviations of the surface plate.

Roto-translation uncertainty

For this method, uncertainty is calculated according to the recommendations of the *Guide to the expression of uncertainty in measurement* (GUM) (Espinosa, Diaz, Baca, Allison, and Shilling, 2008). Equation (15) presents the combined standard uncertainty u_c for the roto-translation method as an estimate of the standard deviation of the possible flatness deviation values. This uncertainty contains all the influence factors that affect the flatness deviations of the surface plate.

$$u_c^2 = u_{res}^2 + u_{rep}^2 + u_{se}^2 + u_{gp}^2 + u_{gb}^2 \tag{15}$$

Here, u_{res} is the uncertainty regarding the resolution of the pin gauges, u_{rep} represents the repeatability of the measurements taken for each grid line, u_{se} denotes the uncertainty of the straight edge, u_{gp} corresponds to the uncertainty of the gauge pins, and u_{gb} is the uncertainty of the gauge blocks.

Method validation

To validate a new method, it is important to determine whether the measurement results fulfill the requirements established for the proposed use. Because of the above, establishing the performance characteristics and limitations related to the measurement process, such as precision, repeatability, limit of detection, and robustness, among others, is the most important task. Measurement methods for flatness calibration have to be capable of ensuring that the results are framed within the tolerances set for surface plates, from grade AA to grade B, and guarantee traceability to the International System of Units (SI) (Drescher, 2003). For the validation process, the roto-translation method was fully developed and optimized; the measurement instruments (the gauge blocks, the gauge pins, and the straight edge) were regularly calibrated, technically controlled, and well maintained (ISO, 2015).

The metrological compatibility model proposed by the VIM3 was employed to validate the roto-translation method (JCGM-BIPM, 2008) because it allows evaluating uncertainty and the precision of each calibrated point. This model calculates the significance of the differences between the results of multiple measurements performed on the same measurand (surface plate). The compatibility test determined whether the results obtained using the roto-translation method could be satisfactorily compared to those of the validated Moody method and could thus be considered acceptable.

To apply the compatibility test, the same surface plate was calibrated using the Moody method via electronic levels. These electronic levels were operated on the pendulum principle, which involves sensing and quantifying the tilt of the level based on the imbalance of the pendulum regarding the reference position. For the flatness calibration of the surface plate, one electronic level remained stationary, while the second one was moved along the grid line presented in Figure 2.

Moody uncertainty

The standard combined uncertainty for the Moody method is presented in Equation 16.

$$u_c^2 = u_{res}^2 + u_{rep}^2 + u_r^2 + u_{el}^2 \tag{16}$$

where u_{res} is the uncertainty regarding the resolution of the electronic levels, u_{rep} denotes the repeatability of the measurements taken for each grid line, u_r corresponds to the uncertainty regarding the rule used to make the grid line diagram on the surface plate, and u_{el} represents the uncertainty of the electronic levels.

Metrological compatibility

NMIs and accredited laboratories report uncertainties with a coverage factor k for the risk of committing an error. Typically, $k = 2$ indicates a confidence of 95% that the measurement results will be within the estimated interval for the reported value (Gromczak *et al.*, 2016). The VIM established that there is metrological compatibility when \the absolute value of the difference of any pair of measured quantity values from two different measurement results is smaller than some chosen multiple of the standard measurement uncertainty of that difference" (Heydorn, 2010). Equation (17) presents the mathematical expression for this definition.

$$|x_i - x_R| \leq \kappa \cdot u_{x_i - x_R} \tag{17}$$

where $|x_i - x_R|$ denotes the absolute error of the method under validation (x_i) with respect to the reference method (x_R), k is the coverage factor and has to be the same for both uncertainties, and $u_{x_i - x_R}$ is the standard uncertainty of the difference between any two quantity values. Equation (18) presents the expression for $u_{x_i - x_R}$.

$$u_{x_i - x_R} = \sqrt{u^2(x_i) + u^2(x_R) - 2r(x_i, x_R)\, u(x_i)\, u(x_R)} \tag{18}$$

where $u(x_i)$ and $u(x_R)$ represent the uncertainty of the under-validation method and the reference method; and the correlation factor between the quantities is denoted as $r(x_i, x_R)$. The calibration methods are independent, making the correlation factor equal to 0. Since the standard expanded uncertainty is $U(x_i) = ku(x_i)$, Equation (17) is usually simplified as presented in Equation (19). This expression is usually known as a *normalized error* (ISO, 2006).

$$E_n = \frac{x_i - x_R}{\sqrt{U^2(x_i) + U^2(x_R)}} \Upsilon \tag{19}$$

A normalized error value between ±1 indicates an acceptable degree of compatibility between the calibration methods. The nearest the value of E_n to 0, the better the compatibility.

Results

To validate the roto-translation method, an A-grade surface plate with a working area of 650×650 mm (ASME-B89.3.7, 2013) was employed as the measurand. For the comparison between calibration methods, we had to ensure that the influence variables affecting the calibration were controlled, so that they did not affect the repeteability and reproducibility of the results. Given the above, the laboratory's environmental conditions were controlled, maintaining a temperature of 20±0.5 °C and a relative humidity of about 50 ±10% Rh (Skattum, 2015).

Moody and electronic levels

The Moody method measurements were taking using two Mahr electronic levels with a foot spacing of L =104.5 mm and expanded uncertainty of U = 0.25 μm. The electronic levels measured the difference between the signals produced by the pendulums to reduce the influence of the vibrations and tilt of the surface plate. Thus, one of the levels acted as a reference and remained stationary at the start of each line of the diagram, and the second was displaced stepwise along the grid lines. The results were stored manually by the calibration operators and were computed in MATLAB, in order to obtain the Moody diagram and its uncertainty. Figure 7 presents all the flatness deviations of the granite surface plate obtained with the Moody method. The advantage of using electronic levels and the Moody method to validate a new measuring method lies in its compatibility and comparability with other, more precise methods, such as those involving auto-colimators and interferometers (Skattum, 2015; Yellowhair and Burge, 2008; Glubokov *et al.*, 2022; Espinosa *et al.*, 2008). Nevertheless, this approach is constrained by the fixed foot spacing of the levels, which limits the measurements to medium and large surface plates (Skattum, 2015; Drescher, 2003).

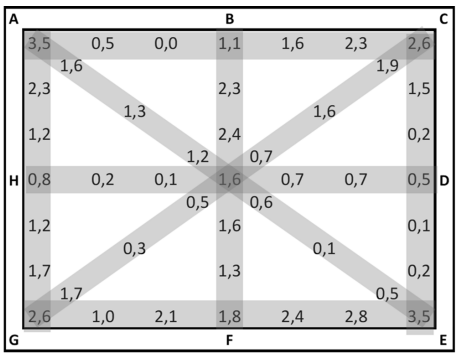

Figure 7. Measurement results obtained with the electronic levels and the Moody method **Source:** Authors

Roto-translation method

To implement the roto-translation method, it is important to properly select the straight edge, since its main purpose is to verify the straightness and flatness of mechanical parts (DIN874-1, 2003). Nevertheless, many of these straight edges are suitable for the verification, measurement, and calibration of surface plates due to their small straight deviations. In light of the above, we used a grade-00 Mahr steel straight edge with a length of 1000 mm, as well as a working edge with a flatness of 7.7 μm and an expanded uncertainty of U=2.7 μm, with a coverage factor k = 2. As a consequence of using different steel measurement instruments (*i.e.*, the gauge pins, the gauge blocks, and the straight edge), it is important to remove the oils used to prevent oxidation, in addition to letting the instruments reach the laboratory temperature on the surface plate. Additionally, during calibration, it is important for the calibrated points of the straight edge to be identified with ruler marks and be properly aligned with the reference calibration points drawn on the surface, in order to prevent measurement errors. Since the surface plate is square, the same calibrated points of the straight edge were used to calibrate the central and perimeter lines, as well as both diagonals (Table 1).

Table 1. Transformations for each vector SE used for measuring the surface plate (μ m)

Grid lines	i	0	1	2	3	4	5	6	7	8
Diagonal lines	SE'	0.0	0.6	3.3	-0.3	-3.2	-0.1	2.5	0.2	0.0
	SE''	0.0	0.6	3.3	-0.3	-3.2	-0.1	2.5	0.2	0.0
Central and perimeter lines	SE'	0.0	0.6	3.8	2.2	-0.8	-3.7	-3.0	-0.1	1.1
	SE''	0.0	0.5	3.5	1.7	-1.4	-4.4	-3.8	-1.1	0.0

Source: Authors

A shown in Table 1, for the diagonal lines, both reference ends of the straight edge were used, thereby avoiding the need to perform any translation or rotation of the vector SE. Following the roto-traslation method, the data for the grid lines, obtained using the gauge pins, was corrected with the vectors SE'' and then rotated and translated (Tables 2,3, and 4). The factors obtained for the rotation and translation of the perimeter lines were $k_{\alpha\beta}$ = 0.1μm and $k_{\alpha\beta}$ -0.3 μm for CE and GE, respectively; and $k_{\beta\alpha}$ =0.1 μm and $k_{\beta\alpha}$ =0.2 μm for AC and AG. For the central lines, BF $k_{\theta\theta'}$ =-0.4 μm and HD $k_{\delta\delta'}$ =0.1 μm were used.

Table 2. Diagonal lines

i	AE	AE^r	AE''	AE^f	CG	CG^r	CG	CG^f
0	0.5	0.5	1.0	3.5	-1.5	-1.5	0.0	2.5
1	-1.3	-1.1	-0.6	1.9	-0.2	-1.9	-0.4	2.2
2	-2.0	-1.7	-1.2	1.4	-1.6	-2.3	-0.8	1.8
3	-1.0	-0.5	0.0	2.5	-0.5	-1.5	0.0	2.5
4	-2.5	-1.8	-1.3	1.2	-1.5	-2.8	-1.3	1.2
5	-3.0	-2.2	-1.7	0.9	0.1	-1.6	-0.1	2.5
6	-0.5	0.5	1.0	3.5	0.5	-1.5	0.0	2.5

Source: Authors

Once the rotations and translations had been performed. We evaluated whether the ends of the diagonals coincided with those of the perimeter lines; whether both ends of the central lines coincided with the central point of the perimeter lines; and whether the center of the central lines coincided with the central point of the diagonals or at least met the criteria of the closure error. Finally, a Moody diagram was elaborated with the results of the final vectors (Figure 8).

Table 3. Central lines

i	BF	BF'	BF''	BF^f	HD	HD'	HD''	HD^f
0	1.1	0.0	-1.6	0.9	0.2	0.0	-1.5	1.0
1	0.5	-0.6	-0.6	1.9	-0.5	-0.7	-1.1	1.5
2	1.1	0.1	0.4	2.9	-0.7	-0.9	-1.4	1.2
3	0.4	-0.7	0.0	2.5	0.7	0.5	0.0	2.5
4	-0.3	-1.4	-0.3	2.2	0.3	0.1	-0.5	2.0
5	-1.9	-3.0	-1.6	0.9	-0.2	-0.4	-1.0	1.5
6	-0.5	-1.5	-1.0	1.6	0.1	-0.1	-2.1	0.4

Source: Authors

Table 4. Perimeter lines

i	AC	AC'	AC''	AC^f	AG	AG'	AG''	AG^f
0	0.5	0.0	1.0	3.5	1.0	0.0	1.0	3.5
1	-1.5	-2.1	-1.2	1.3	0.0	-1.1	-0.2	2.3
2	-1.7	-2.3	-1.6	1.0	-0.4	-1.5	-0.8	1.7
3	-1.7	-2.2	-1.6	0.9	-1.,0	-2.0	-1.5	1.0
4	-0.6	-1.,2	-0.7	1.8	0.4	-0.7	-0.3	2.2
5	0.8	0.3	0.6	3.1	0.8	-0.2	-0.1	2.5
6	0.4	-0.1	0.0	2.5	1.,1	0.,0	0.0	2.5
i	CE	CE'	CE''	CE^f	GE	GE'	GE''	GE^f
0	-0.5	0.0	0.0	2.5	1.2	0.,0	0.0	2.5
1	-0.5	-0.,1	-0.2	2.4	-0.5	-1.7	-1.4	1.1
2	-1.7	-1.3	-1.5	1.1	0.8	-0.4	0.2	2.8
3	-2.3	-1.8	-2.1	0.4	-0.7	-1.9	-1.0	1.6
4	-1.6	-1.2	-1.5	1.0	1.4	0.2	1.4	3.9
5	-2.5	-2.0	-2.5	0.0	1.4	0.2	1.7	4.3
6	1.1	1.6	1.0	3.5	0.,4	-0.,8	1.0	3.5

Source: Authors

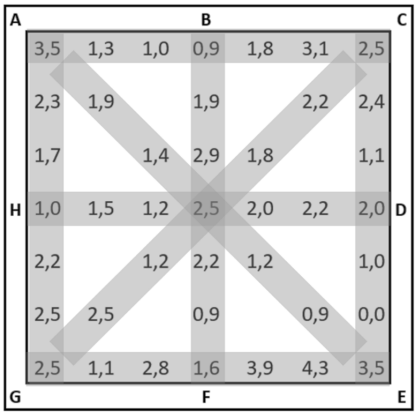

Figure 8. Measurement results obtained with the roto-translation method **Source:** Authors

Evaluating measurement uncertainty

Table 5 presents the uncertainty evaluation of the roto-translation method, which was carried out using Equation (15. Note that the straight edge ($u(se)$) is the factor with the greatest influence on the roto-translation's expanded uncertainty. In this work, the straight edge was calibrated using a CMM with high uncertainty. However, if required, this parameter can be reduced by calibrating the straight edge through a different measuring system or method with less uncertainty.

For the uncertainty evaluation of the Moody method, Equation (16) was used. The results are presented in Table 6.

Table 5. Uncertainty estimation for the roto-translation method

Source of uncertainty	$u(x_i)$	Units	c_i	ν_i	$(u(x_i)\times c_i)$
Resolution	$u(res)=\frac{res}{2\sqrt{3}}$	μm	1	50	0.29
Repeatability	$u(rep)=\frac{s_p}{\sqrt{n}}$	μm	1	2	0.33
Straight Edge	$u(SE)=\frac{U_{SE}}{k}$	μm	1	200	1.35
Gauge Pin	$u(gp)=\frac{U_{gp}}{k}$	μm	1	200	0.40
Gauge Block	$u(gb)=\frac{U_{gb}}{k}$	μm	1	200	0.02
Expanded uncertainty, ($k=2$)					**2.9 μm**

Source: Authors

Table 6. Uncertainty estimation for the Moody method

Source of uncertainty	$u(x_i)$	Units	c_i	ν_i	$(u(x_i)\times c_i)$
Resolution	$u(res)=\frac{res}{2\sqrt{3}}$	μm	1	50	0.01
Repeatability	$u(rep)=\frac{s_p}{\sqrt{n}}$	μm	1	2	0.30
Electronic Levels	$u(SE)=\frac{U_{el}}{k}$	μm	1	200	0.13
Ruler	$u(r)=\frac{\sqrt{(u_c c_c)^2+(u_\alpha c_\alpha)^2+(u_\theta c_\theta)^2}}{L}$	μm	1	200	0.0001
Expanded uncertainty, ($k=2$)					**1,1 μm**

Source: Authors

Table 6 shows that the Moody expanded uncertainty is influenced by the ruler used to trace the lines of the diagram, and that it is composed of the uncertainty of the ruler u_c, the uncertainty of the ruler coefficient of thermal expansion u_α, the laboratory temperature u_θ, and the distance between the centers of the electronic level feet L. It is important to consider this uncertainty since it directly influences the steps in which the electronics levels take measurements to estimate the deviation of each calibration point in the grid line diagram.

For both methods, *flatness* was defined as the distance between the base plane and the roof plane (Novyanto and Pratiwi, 2016; Skattum, 2015).

Table 7. Uncertainty estimation for each measurement method

Measurement Method	Flatness [μm]	Closure error		Uncertainty [μm]
		BF[μm]	HD[μm]	
Roto-translation	4.3	-1.2	-1.1	2.9
Moody	3.5	-2.3	-1.9	1.1

Source: Authors

Based on Table 7, it is important to note that the flatness results obtained with both methods are comparable, despite the fact that the resolution of the gauge pins ($\pm 1\mu$m) is 20 times higher than that of the electronic levels (0.05μm). Nevertheless, uncertainty entailed a great difference between both methods; the uncertainty of the roto-traslation was higher than that of the Moody method. This uncertainty is suitable for the calibration and verification of surface plates in the industry and in small laboratories, as has been previously reported (ASME-B89.3.7, 2013; ISO8512-2, 1990; Zahwi, Amer,

Abdou, and Elmelegy, 2013; Skattum, 2015). The closure error obtained for both methods is an important criterion for correcting the measurements, as it indicates potential issues associated with personnel, the measurement system, or the surface plate. Finally, the flatness values obtained with both methods range from 3.5 μm to 4.3 μm, meeting the grade-A flatness specifications for surface plates of this size (ASME-B89.3.7, 2013).

Validating the roto-translation method

To compare the results shown in Figures 7 and 8, each grid line result was represented with its uncertainty bars (Figures 9 and 10). These Figures demonstrate that both methods describe the same surface plate point by point, regardless of the differences in resolution and uncertainty.

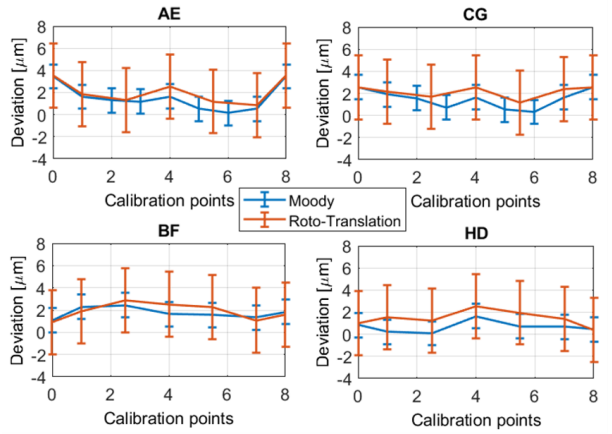

Figure 9. Validation of the roto-translation method with regard to the diagonals and central lines **Source:** Authors

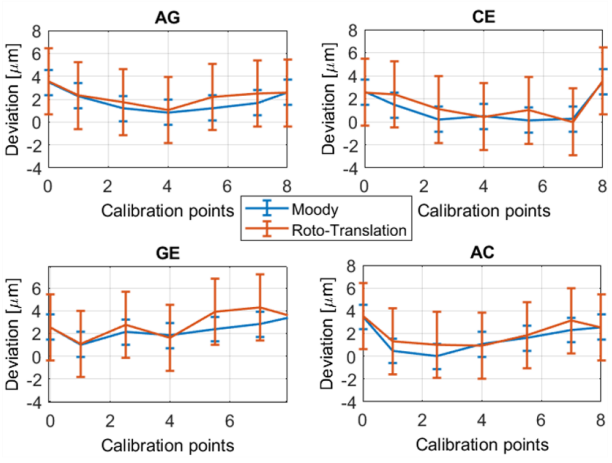

Figure 10. Validation of the roto-translation method with regard to perimeter lines **Source:** Authors

As shown in Figures 9 and 10, the flatness deviation variations between methods are most likely associated with the differences between the measurement systems, with the error introduced by the individual carrying out the calibration, and with the fact that the measurement points can slightly differ between methods because the gauge pins have to be placed exactly in each point of the grid lines. Meanwhile, for the electronic levels, the deviation of each point is estimated via geometric calculations.

To validate the results obtained with the roto-translation method, the normalized error E_n was calculated, using Equation (19) to evaluate the consistency of each calibration point of the Moody diagram (Zahwi *et al.*, 2013), as shown in Table 8.

Table 8. Estimation of the normalized error

	Normalized error							
i	AE	CG	AC	CE	GE	AG	BF	HD
0	0.01	-0.02	0.03	-0.01	-0.01	0.03	-0.04	0.06
1	0.08	0.09	0.26	0.27	0.02	0.00	-0.11	0.38
2	0.05	0.19	0.29	0.26	0.18	0.17	0.14	0.32
3	0.26	0.26	-0.04	-0.01	-0.07	0.06	0.27	0.27
4	0.25	0.23	0.06	0.26	0.45	0.29	0.19	0.38
5	0.11	0.25	0.24	-0.07	0.44	0.23	-0.12	0.25
6	0.01	-0.02	-0.01	0.03	0.03	-0.01	-0.07	-0.01

Source: Authors

As observed in Table 8, the E_n values are within the range of ±1 for all measured points. It could be said that there are no significant differences between the measured flatness deviations found by both methods. Given the above, the roto-traslation method is compatible with and comparable to the Moody method, and it can be used for calibrating and verifying grade-AA surface plates with dimensions over 609×1219 mm, grade-A plates with dimensions over 457×609 mm, and grade-B surface plates with dimensions over 305×457 mm (ASME-B89.3.7, 2013).

Conclusions

In validating the proposed roto-traslation method, we found that it is important to allow the surface plate, gauge pins, straight edge, and blocks to reach thermal stability, as this can directly affect the repeatability and reproducibility of the results (Skattum, 2015). Additionally, the uncertainty of this method is suitable for calibrations and intermediate verifications; it meets the requirements for the measurement and calibration of surface plates of grades AA to B (ASME-B89.3.7, 2013; Drescher, 2003). In Table 8, the normalized error reveals a bias that is sufficiently small in relation to the Moody method, demonstrating a point-by-point metrological compatibility between methods. Given the above, the roto-translation method can be recommended to laboratories that require constant verification of the state of surface plates, surfaces, large lenses, and mirrors (Yellowhair and Burge, 2008), as it implies a lower economic investment (*i.e.*, instrument purchasing and technical maintenance).

The expanded uncertainty obtained with the Moody method was U= 1.1μ m, with a coverage factor k = 2. According to the documentation (ASME-B89.3.7, 2013) for a grade-A surface plate of 24 × 24 (*i.e.* 609.6 × 609.6 mm), the overall flatness has to be 160μin (*i.e.*, 4,06 μm). Thus, the flatness results obtained with the Moody method are within the standard specifications.

As part of the calibration procedure with the roto-translation method, we found that the straightness ruler marks have to be perfectly aligned with the reference surface calibration points, as this directly influences the results and can cause the closing error to be greater than 2.5 μm. This was proven by different technical professionals of the laboratory, and it directly affected the reproducibility of the method.

Since the accuracy of the measurement instruments employed by the roto-translation method is lower than that of electronics levels, there is a magnitude difference between the uncertainties presented in Table 7 and Figure 8. Since the straight edge was calibrated with a CMM, its uncertainty is the most significant component in the uncertainty model of the roto-translation method.

With the results presented in this work, the research team means to encourage new and small laboratories to use this method to calibrate and characterize their surface plates.

Acknowledgments

This work was carried out within the framework of the project titled *Plan for strengthening the INM as a research center* (code 9932100271370), funded by the Ministry of Science, Technology, and Innovation (Minciencias) and jointly executed by the INM and Universidad Nacional de Colombia through the Special Cooperation Agreement 001 of 2020.

CRedit author statement

Daniela I. Garzon carried out most of the experiments, collected all the data for the formal analysis, and developed software programs and applications for data processing and results visualization. Jorge L. Galvis conceived the idea and did the background research, supervised the research, provided critical feedback, and led the research and the validation process. David A. Plazas carried out all the calibrations of the measurement instruments used during the experiments and participated in the validation process. Victor H. Gil designed the first approximation to the measurement method and participated in the validation process. Ovidio Almanza reviewed, supported, and oversaw the research process.

Conflicts of interest

The authors declare no conflict of interest.

References

Ali, S. H., and Buajarern, J. (2013, Dec). New measurement method and uncertainty estimation for plate dimensions and surface quality. *Advances in Materials Science and Engineering*, *2013*, 1-10 https://doi.org/10.1155/2013/918380.

ASME-B89.3.7. (2013). *B89.7.3. Granite Surface Plates*. ASME.

Azaryan, N., Budagov, J., Gayde, J.-C., Girolamo, B. D., Glagolev, V., Lyablin, M., ... Shirkov, G. (2017, 1). The innovative method of high accuracy interferometric calibration of the precision laser inclinometer. *Physics of Particles and Nuclei Letters*, *14*, 112-122 http://link.springer.com/10.1134/S154747711701006X.

DIN874-1. (2003). Geometrical product specifications (gps) - straight edges - part 1: Steel straight edges; dimensions, technical delivery conditions. *DIN 874-1:2003-11*, *2003*.

Drescher, J. (2003). Analytical estimation of measurement uncertainty in surface plate calibration by the moody method using differential levels. *Precision engineering*, *27*(3), 323–332.

Ehret, G., Reinsch, H., and Schulz, M. (2019). Interferometric and deflectometric flatness metrology with nanometre measurement uncertainties for optics up to 1 metre at PTB. In S. Han, T. Yoshizawa, S. Zhang, and B. Chen (Eds.), *Optical metrology and inspection for industrial applications vi* (Vol. 11189, p. 1118905 https://doi.org/10.1117/12.2538872.). SPIE.

Ehret, G., Schulz, M., Fitzenreiter, A., Baier, M., Jockel, W., Stavridis, M., and Elster, C. (2011). Alignment methods for ultraprecise deflectometric flatness metrology. In P. H. Lehmann, W. Osten, and K. Gastinger (Eds.), *Optical measurement systems for industrial inspection vii* (Vol. 8082, p. 808213 https://doi.org/10.1117/12.889325.). SPIE.

Espinosa, O. C., Diaz, P., Baca, M. C., Allison, B. N., and Shilling, K. M. (2008). *Comparison of calibration methods for a surface plate*. (Tech. Rep.). Sandia National Lab.(SNL-NM), Albuquerque, NM (United States).

Geckeler, R. D., Schumann, M., Just, A., Krause, M., Lassila, A., and Heikkinen, V. (2022, feb). A comparison of traceable spatial angle autocollimator calibrations performed by ptb and vtt mikes. *Metrologia*, *59*(2), 024002 https://dx.doi.org/10.1088/1681-7575/ac42b9.

given i=K., f., given=Kouyu. (n.d.). On a method for measuring flatness by two-point connecting method. , *8*(30), 274–280 http://dx.doi.org/10.1299/jsme1958.8.274.

Glubokov, A., Glubokova, S., Afonina, I., Zelensky, A., and Semenishchev, E. A. (2022, 12). Automated measuring system for straightness and flatness deviations of extended surfaces. *Optical Metrology and Inspection for Industrial Applications IX* http://dx.doi.org/10.1117/12.2646259..

Gromczak, K., Gąska, A., Kowalski, M., Ostrowska, K., Sładek, J., Gruza, M., and Gąska, P. (2016, dec). Determination of validation threshold for coordinate measuring methods using a metrological compatibility model. *Measurement Science and Technology*, *28*(1), 015010 https://dx.doi.org/10.1088/1361-6501/28/1/015010.

Gusel, A., Acko, B., and Sostar, A. (2000a). Assuring the traceability of electronic levels for calibration of granite surface plates. In *Proc. xvi imeko world congress*.

Gusel, A., Acko, B., and Sostar, A. (2000b). Assuring the traceability of electronic levels for calibration of granite surface plates. In *Proc. xvi imeko world congress*.

Heikkinen, V., Byman, V., Palosuo, I., Hemming, B., and Lassila, A. (2017, 6). Interferometric 2d small angle generator for autocollimator calibration. *Metrologia*, *54*, 253-261 https://iopscience.iop.org/article/10.1088/1681-7575/aa648d.

Heydorn, K. (2010, Nov 01). Metrological compatibility a key issue in future accreditation. *Accreditation and Quality Assurance*, *15*(11), 643-645 https://doi.org/10.1007/s00769-010-0691-8.

ISO. (2006). Guide iso/cei 99 2007 vocabulaire international de métrologie concepts fondamentaux et généraux et termes associés (vim). *Vocabulary*, *2007*(VIM), 1–150.

ISO. (2015). Statistical methods for use in proficiency testing by interlaboratory comparison. *Iso 13528,*, *2015*.

ISO8512-2. (1990). Surface plates-part 2: Granite. *ISO 8512-2*, *1990*.

JCGM-BIPM. (2008). Evaluation of measurement data | guide to the expression of uncertainty in measurement. *Int. Organ. Stand. Geneva ISBN*, *50*(September), 134.

Ju HUO, M. Y., Yunhui LI. (2018). Multi-channel signal parameters joint optimization for gnss terminals. *Journal of Systems Engineering and Electronics*, *29*(4), 844. https://dx.doi.org/10.21629/JSEE.2018.04.19. Retrieved from https://www.jseepub.com/EN/abstract/article_6421.shtml

Lakota, S., and Gorog, A. (2011). Flatness measurement by multi-point methods and by scanning methods. *Ad Alta: Journal of Interdisciplinary Research*, *1*(1), 124–127.

Meijer, J., and Heuvelman, C. (1990). Accuracy of surface plate measurements|general purpose software for flatness measurement. *CIRP annals*, *39*(1), 545–548.

Mikó, B. (2021, 2). Assessment of flatness error by regression analysis. *Measurement*, *171*, 108720 http://dx.doi.org/10.1016/j.measurement.2020.108720.

Moody, J. (1955). How to calibrate surface plates in the plant. *The Tool Engineer*, *1955*, 85–91.

Novyanto, O., and Pratiwi, E. (2016). A preliminary study to evaluate the topography of narrow surface plate. *Instrumentasi*, *39*(1), 1–8 https://jurnalinstrumentasi.bsn.go.id/index.php/ji/article/view/67.

Schulz, M., Ehret, G., and Křen, P. (2013). High accuracy flatness metrology within the european metrology research program. *Nuclear Instruments and Methods in Physics Research Section A: Accelerators, Spectrometers, Detectors and Associated Equipment*, *710*, 37-41. https://doi.org/10.1016/j.nima.2012.10.112. Retrieved from https://www.sciencedirect.com/science/article/pii/S0168900212012855 (The 4th international workshop on Metrology for X-ray Optics, Mirror Design, and Fabrication)

Skattum, G. A. (2015, Mar). Estimating thermal effects for granite surface plate calibration. *NCSLI Measure*, *10*(1), 50–58 https://dx.doi.org/10.1080/19315775.2015.11721716.

Yang, Y., Wang, T., and Zhu, G. (2021, jul). Calibration method for the bubble angle of inclination for the spirit levels based on the calibration device. *Journal of Physics: Conference Series*, *1982*(1), 012160 https://dx.doi.org/10.1088/1742-6596/1982/1/012160.

Yellowhair, J., and Burge, J. H. (2008). Measurement of optical flatness using electronic levels. *Optical Engineering*, *47*(2), 023604 https://doi.org/10.1117/1.2831131.

Zahwi, S., Amer, M., Abdou, M., and Elmelegy, A. (2013). On the calibration of surface plates. *Measurement*, *46*(2), 1019-1028. https://doi.org/10.1016/j.measurement.2011.10.009. Retrieved from https://www.sciencedirect.com/science/article/pii/S0263224111003551